

AUTONOMOUS MANEUVERS OF A FARM VEHICLE WITH A TRAILED IMPLEMENT IN HEADLAND

Christophe Cariou, Roland Lenain, Michel Berducat
Cemagref, UR TSCF, 24 avenue des Landais, 63172 Aubière, France

Benoit Thuilot
Clermont Université, Université Blaise Pascal, LASMEA, BP 10448, 63000 Clermont-Ferrand, France

Keywords: Guidance system, Mobile robot, Path planning, Motion control, Agriculture.

Abstract: This paper addresses the problem of path generation and motion control for the autonomous maneuvers of a farm vehicle with a trailed implement in headland. A reverse turn planner is firstly investigated, based on primitives connected together. Then, both steering and speed control algorithms are considered. When the system is driving forward, the control algorithms are based on a kinematic model extended with additional sliding parameters and on model predictive control approaches. When the system is driving backward, two different steering controllers are proposed and compared. Real world experiments have been carried out with an experimental trailer hitched to a mobile robot. At the end of each row, the reverse turn is automatically generated to connect the next reference track, and the maneuvers are autonomously performed. Reported experiments demonstrate the capabilities of the proposed algorithms.

1 INTRODUCTION

For many years, researchers and manufacturers have widely pointed out the benefits of developing automatic guidance systems for agricultural vehicles, in particular to improve field efficiency while releasing human operator from monotonous and dangerous operations. Auto-steering systems are becoming common place (e.g. *Agco AutoGuide*, *Agrocom E-drive*, *Autofarm AutoSteer*, *Case IH AccuGuide*, *John-Deere AutoTrac*) and focus on accurately following parallel tracks in the field. However, more advanced functionalities are today required, in particular for headland driving. In fact, the operator must still manually perform maneuvers at the end of each row before reengaging the automatic guidance system on the next path to follow. In order to benefit of fully automated solutions, and therefore reduce the operator's workload (and even enable to consider driverless agricultural vehicles), the automation of the maneuvers in headland has to be studied with meticulous care.

Very few approaches have been proposed in that way, mainly based on loop turns (e.g. *John-Deere iTEC Pro*, see figure 1(a)). The drawback of such an approach is that it involves excessive headland width

for turning on the adjacent track, all the more if a long trailer is used. It is thereby not adapted for small fields and far from optimal in term of productivity, headland being usually either low-yield field areas due to high soil compaction or wasted areas as they cannot be used for planting agricultural products.



(a) Loop turn. (b) Fish-tail. (c) With trailer.

Figure 1: Different types of maneuver in headland.

Another solution is to perform reverse turns, i.e. maneuvers executed with stop points and a reverse motion as depicted in figures 1(b) and 1(c), leading to reduced headlands. However, although more in accordance with European agricultural practices, automation of such maneuvers in headland has rarely been considered in the literature. In fact, numerous approaches devoted to road applications have been proposed for the autonomous maneuvers of a vehicle, even with one or several trailers, see (Altafini C., 2001), (Lamiroux F., 1998), (Hermosillo J., 2003),

but most of these control algorithms seem not well-adapted for an agricultural context. This paper proposes to address the automation of the maneuvers of a vehicle-trailer system, dedicated to an off-road context. This paper extends our previous work (Cariou et al., 2009) where accurate fish-tail maneuvers without trailer were autonomously performed. The general 1-trailer system is here considered, i.e. the trailer is hitched up at some distance from the middle point of the rear axle of the vehicle.

2 MOTION PLANNER

With regard to the path planning problem of agricultural machines in headland, generic optimal control algorithms are often investigated to find optimal point-to-point trajectories for a given cost function from a wide variety of configurations, see (Vougioukas et al., 2006). Primitive-based planning approaches are also widely used in the literature, relying either on clothoids, polynomial splines or cubic spirals to construct non-holonomic motions, see (Lau B., 2009). We have studied a similar approach well-adapted to agricultural maneuvers. It allows to rapidly obtain an efficient path planning solution for reverse turns of a vehicle-trailer system, based on elementary primitives (line segment, arc of circle) connected together with pieces of clothoid in order to ensure curvature continuity.

2.1 Arc of Clothoid

The curvature c of a clothoid varies linearly with respect to its curvilinear abscissa s ($c = g \cdot s$), see figure 2. An arc of clothoid BP_1 admissible for the considered vehicle can then be defined in order to connect a line segment AB to a circle of radius R . To avoid the saturation of the steering actuator, R is chosen slightly upper than the minimum curvature radius of the vehicle. The proportionality coefficient g is computed according to the maximum vehicle front-wheel angular velocity ($\omega_a = 20^\circ/s$) and of the vehicle linear velocity ($v_{ref} = 1.75m/s$) during the reverse turn, see (Cariou et al., 2009) for more details. In that way, continuous curvature trajectories admissible for the vehicle can easily be constructed.

2.2 Trajectory Generation Strategy

The aim is to connect two adjacent tracks AB and CD separated from a distance d , see figure 3(a). The proposed strategy considers the following motions.

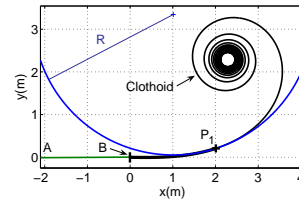


Figure 2: Clothoid, $g = 0.15$.

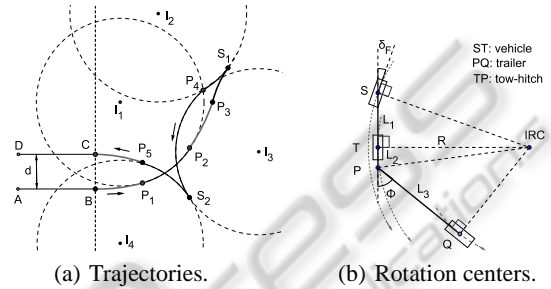


Figure 3: Path planning.

- The first movement from B to S_1 is composed of an arc of clothoid BP_1 , to increase the curvature from $c = 0$ to $c = \frac{1}{R}$, an arc of circle P_1P_2 of center I_1 and of radius R , a second arc of clothoid P_2P_3 to decrease the curvature from $c = \frac{1}{R}$ to $c = 0$, and a part of a third arc of clothoid P_3S_1 required to align the trailer with the vehicle at the end of the movement. Aligning the vehicle-trailer system at the first stop point S_1 leads to a suitable configuration to plan the reverse motion. At S_1 , the wheels are reorientated to change the vehicle instantaneous rotation center to I_2 .
- The reverse movement is then built, composed firstly of an arc of circle S_1P_4 to increase the vehicle-trailer angle ϕ , see the notation in the bicycle representation figure 3(b). The point P_4 is determined in order that the vehicle-trailer system reaches the configuration shown in figure 3(b): the center of rotation of the trailer coincides with the center of rotation of the vehicle, when the vehicle front steering angle is set to a value $\delta_F^d = 20^\circ$. Geometrical considerations show that the expected value ϕ_{ref} for the angle ϕ is:

$$\phi_{ref} = \pi - \arctan\left(\frac{R}{L_2}\right) - \arccos\left(\frac{L_3}{\sqrt{R^2 + L_2^2}}\right) \quad (1)$$

with: $R = L_1 / \tan \delta_F^d$

This is a stable configuration enabling a circular motion of radius R when pure rolling without sliding conditions are satisfied. It serves here as an objective configuration. At P_4 , the wheels are reorientated to change the vehicle instantaneous ro-

tation center from I_2 to I_3 . Then, an arc of circle P_4S_2 of center I_3 and radius R is built.

- The third movement is composed of an arc of circle S_2P_5 of center I_4 and radius R , and an arc of clothoid P_5C to decrease the curvature from $c = \frac{1}{R}$ to $c = 0$. S_2 is the second stop point, defined as the intersection between the circles of center I_3 and I_4 .

Figure 4 presents simulation results with two adjacent tracks separated from a distance $d = 2m$. At the first stop point S_1 , the vehicle-trailer angle is $\phi = 0^\circ$, i.e. the trailer and the vehicle are aligned, see the trajectories of points S , T and Q , respectively the centers of the vehicle front and rear axle and the center of the trailer axle. During the reverse motion, the vehicle-trailer angle reaches and maintains the expected configuration ϕ_{ref} (here $\phi_{ref} = 53^\circ$).

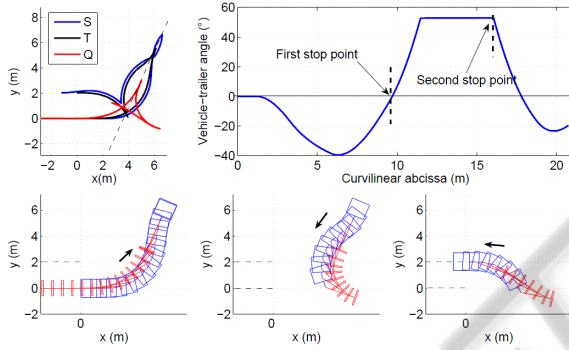


Figure 4: Path planning results.

3 CONTROL ALGORITHMS

3.1 Forward Motion

Accurate automatic guidance of mobile robots in an agricultural environment constitutes a challenging problem, mainly due to the low grip conditions usually met in such a context. In fact, as pointed out in (Wang D., 2006), if the control algorithms are designed from pure rolling without sliding assumptions, the accuracy of path tracking may be seriously damaged, especially in curves. Therefore, sliding has to be accounted in the control design to preserve the accuracy of path tracking, whatever the path to be followed and soil conditions.

3.1.1 Kinematic Model extended with Sliding Parameters

In the same way than in (Lenain et al., 2006a), two parameters homogeneous with sideslip angles in a dynamic model, are introduced to extend the classical

kinematic model, see the bicycle representation of the vehicle in figure 5. These two angles, denoted β_F and β_R for the front and rear axle, represent the difference between the theoretical direction of the linear velocity vector at wheel centers, described by the wheel plane, and their actual direction. These angles are assumed to be entirely representative of sliding influence on vehicle dynamics. The notations used in this paper are listed below and depicted in figure 5.

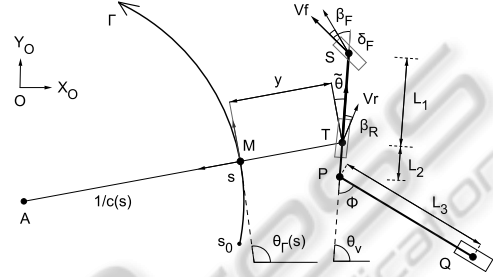


Figure 5: Path tracking parameters.

- S and T are the centers of the front and rear virtual wheel. T is the point to be controlled.
- θ_v is the orientation of vehicle centerline with respect to an absolute frame $[O, X_O, Y_O]$.
- δ_F is the front steering angle and constitutes the first control variable.
- V_r is the vehicle linear velocity at point T and constitutes the second control variable.
- β_F and β_R are the front and rear sideslip angles.
- M is the point on the reference path Γ to be followed, which is the closest to T .
- s is the curvilinear abscissa of point M along Γ .
- $c(s)$ is the curvature of the path Γ at point M .
- $\theta_\Gamma(s)$ is the orientation of the tangent to Γ at point M with respect to the absolute frame $[O, X_O, Y_O]$.
- $\tilde{\theta} = \theta_v - \theta_\Gamma$ is the vehicle angular deviation.
- y is the vehicle lateral deviation at point T .
- ϕ is the vehicle-trailer angle.
- $L_1 = 1.2m$ and $L_3 = 2.34m$ are respectively the vehicle and trailer wheelbases. $L_2 = 0.46m$ is the vehicle tow-hitch.

The equations of motion are derived with respect to the path Γ . It can be established, see (Lenain et al., 2006a), that:

$$\begin{cases} \dot{s} = V_r \frac{\cos(\tilde{\theta} - \beta_R)}{1 - c(s)y} \\ \dot{y} = V_r \sin(\tilde{\theta} - \beta_R) \\ \dot{\tilde{\theta}} = V_r [\cos(\beta_R)\lambda_1 - \lambda_2] \\ \dot{\phi} = -\frac{V_r}{L_1 L_3} [\tan \delta_F (L_2 \cos \phi + L_3) + L_1 \sin \phi] \end{cases} \quad (2)$$

$$\text{with: } \lambda_1 = \frac{\tan(\delta_F - \beta_F) + \tan(\beta_R)}{L_1}, \lambda_2 = \frac{c(s)\cos(\tilde{\theta} - \beta_R)}{1 - c(s)y}$$

Model (2) accurately describes the vehicle motion in presence of sliding as soon as the two additional parameters β_F and β_R are known. An observation algorithm has been developed to achieve indirect estimation, relying on the sole lateral and angular deviation measurements, see (Lenain et al., 2006b).

3.1.2 Control Law Design

The extended model (2) constitutes a relevant basis for mobile robot control design. As the vehicle-trailer system is well-known for being naturally exponentially stable when driving forward, the trailer is ignored in this case. In (Lenain et al., 2006a), the first three equations in model (2) have been converted in an exact way into linear equations, according to the state and control transformations:

$$\begin{aligned} [s, y, \tilde{\theta}] &\rightarrow [a_1, a_2, a_3] = [s, y, (1 - c(s)y) \tan(\tilde{\theta} + \beta_R)] \\ [V_r, \delta_F] &\rightarrow [m_1, m_2] = \left[\frac{V_r \cos(\tilde{\theta} + \beta_R)}{1 - c(s)y}, \frac{da_3}{dt} \right] \end{aligned} \quad (3)$$

Finally, if derivatives are expressed with respect to the curvilinear abscissa, the following chained form is obtained:

$$\begin{cases} a_2' = \frac{da_2}{da_1} = a_3 \\ a_3' = \frac{da_3}{da_1} = m_3 = \frac{m_2}{m_1} \end{cases} \quad (4)$$

Since chained form (4) is linear, a natural expression for the virtual control law m_3 is:

$$m_3 = -K_d a_3 - K_p a_2 \quad (K_p, K_d) \in \mathfrak{R}^{+2} \quad (5)$$

since it leads to:

$$a_2'' + K_d a_2' + K_p a_2 = 0 \quad (6)$$

which implies that both a_2 and a_3 converge to zero, i.e. $y \rightarrow 0$ and $\tilde{\theta} \rightarrow \beta_R$. The inversion of control transformations provides the front steering control law:

$$\delta_F = \beta_F + \arctan \left\{ -\tan(\beta_R) + \frac{L_1}{\cos(\beta_R)} \left(\frac{c(s)\cos\tilde{\theta}_2}{\alpha} + \frac{A\cos^3\tilde{\theta}_2}{\alpha^2} \right) \right\} \quad (7)$$

$$\text{with: } \begin{cases} \tilde{\theta}_2 = \tilde{\theta} - \beta_R \\ \alpha = 1 - c(s)y \\ A = -K_p y - K_d \alpha \tan\tilde{\theta}_2 + c(s)\alpha \tan^2\tilde{\theta}_2 \end{cases}$$

In addition, as the actuation delays and vehicle inertia may lead to significant overshoots, especially at each beginning/end of curves, a predictive action must be added to the steering control in order to maintain accurate path tracking performances, see (Lenain

et al., 2006b) for more details. A second control loop can be designed, dedicated to speed control. In (Cariou et al., 2009), a Model Predictive Control technique is used to anticipate speed variations and reject significant overshoots in longitudinal motion.

3.2 Backward Motion

It is well-known that steering backward a vehicle-trailer system has a tendency to jackknife, and requires special driving skill. In the literature, numerous path following approaches have addressed this problem when the trailer is hooked directly at the center of the rear axle of the vehicle. In contrast, the case of deported trailers has been rarely considered. In this paper, we propose to indirectly control the vehicle-trailer angle. Two control strategies are proposed.

3.2.1 Regulation of the Vehicle-trailer Angle

With the motion planner described in subsection 2.2, the previous steering control law (7) can be used during the backward motion until the vehicle-trailer system presents the expected angle ϕ_{ref} , corresponding to the configuration at point P_4 depicted in figure 3(b). Next, as the rest of the backward movement is quite short to reach the stop point S_2 , the vehicle-trailer angle can be simply stabilized on ϕ_{ref} . More precisely, relying on the fourth equation in model (2), the error dynamic $\dot{\phi} = K_R(\phi_{ref} - \phi)$ ($K_R > 0$) can be imposed with the following front-wheel steering control law:

$$\delta_F = \arctan \frac{-L_1 \sin \phi - \frac{K_R L_1 L_3 (\phi_{ref} - \phi)}{V_r}}{L_2 \cos \phi + L_3} \quad (8)$$

3.2.2 Stabilization of the Trailer on the Planned Trajectory

Another solution is to control the center of the trailer axle on its respective planned trajectory, see the trajectory of Q during the backward motion in figure 4. For that, the trailer is first considered as an independent virtual vehicle, with a rear steering wheel located at the hitch point P and a fixed front-wheel located at point Q , see figure 6. The control objective can then be expressed as ensuring the convergence of this virtual vehicle (moving forward) to the reference path Γ . The first three equations in model (2) describe the motion of such a vehicle, except that δ_F has to be replaced by $-\delta_c$, since the variations in the orientation of the vehicle are inverted when rear steering is considered instead of front steering. The state variables are now y_t and $\tilde{\theta} = \theta_t - \theta_\Gamma$, respectively the trailer lateral and angular deviation, see figure 6. A chained form transformation similar to the one presented in

subsection 3.1 can then be applied, and the expected value for δ_c can be directly inferred from (7):

$$\delta_c = -\arctan \left\{ L_3 \left(\frac{c(s) \cos \tilde{\theta}}{\alpha_t} + \frac{A_t \cos^3 \tilde{\theta}}{\alpha_t^2} \right) \right\} \quad (9)$$

$$\text{with: } \begin{cases} \alpha_t = 1 - c(s)y_t \\ A_t = -K_p y_t - K_d \alpha_t \tan \tilde{\theta} + c(s) \alpha_t \tan^2 \tilde{\theta} \end{cases}$$

δ_c describes the desired direction of the linear velocity \vec{v} at the hitch point. Then, the vehicle-trailer angle ϕ_{ref} ensuring that the center of rotation of the trailer coincides with the center of rotation of the vehicle can easily be inferred from δ_c via basic geometrical relations, see figure 6:

$$\phi_{ref} = \delta_c + \arcsin \frac{L_2 \sin \delta_c}{L_3} \quad (10)$$

Finally, the proposed angle ϕ_{ref} can be controlled just as in subsection 3.2.1: reporting (10) into (8) provides the front steering control law for the vehicle.

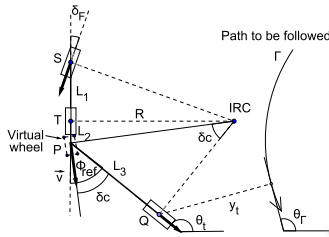


Figure 6: Trailer as a virtual vehicle.

4 EXPERIMENTAL RESULTS

In this section, the capabilities of the proposed control algorithms are investigated on an irregular natural terrain, using the experimental vehicle-trailer system depicted in figure 7. The vehicle is an all-terrain mobile robot whose weight is 650kg. The only exteroceptive sensor is an RTK-GPS receiver, whose antenna has been located straight up the center of the vehicle rear axle. It supplies an absolute position accurate to within 2cm, at a 10Hz sampling frequency. The vehicle-trailer angle is measured using a potentiometer. A gyrometer has also been added to obtain an accurate heading of the vehicle during the maneuvers.

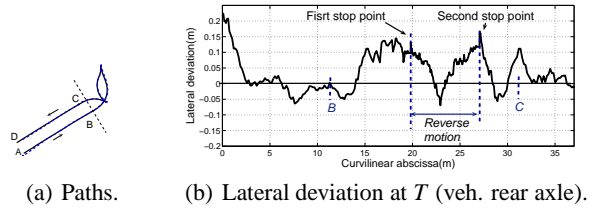
In the forthcoming experimental test, the objective for the vehicle-trailer system is to follow autonomously two straight lines AB and CD separated from $2m$, see figure 8(a), and to execute autonomously the reverse turn using control law (8). The lateral deviation recorded at the center T of the rear wheels, according to the curvilinear abscissa, is



Figure 7: Experimental vehicle-trailer system.

reported in figure 8(b). At the beginning, the vehicle starts at about $25cm$ from the path to be followed. Then, it reaches the planned path and maintains an overall lateral error about $\pm 15cm$ during the maneuver. The main overshoots in the lateral deviation take place at the moment of a large deceleration and acceleration on a sliding ground (curvilinear abscissas $15m$ and $32m$). Despite such conditions, the lateral deviation remains inside $\pm 15cm$. This highlights the capabilities of the proposed algorithms, taking into account for sliding effects and actuator delays.

The vehicle speed is reported at the top of figure 9. The speed reference $v_{ref} = 1.75m/s$ is correctly followed, and the speed variations are satisfactorily anticipated with the predictive approach. At the center of figure 9 is reported the vehicle front steering angle. It can be observed that its variations are quite smooth and that the wheels are satisfactorily reorientated to change the vehicle instantaneous rotation center at the stop points as well as at point P_4 (curvilinear abscissa $22m$). The vehicle-trailer angle w.r.t. the curvilinear abscissa is reported at the bottom of figure 9. In accordance with the simulations depicted in figure 4, this angle reaches -40° during the first movement. The trailer and the vehicle are then aligned at the first stop point. During the reverse motion, this angle increases up to $\phi_{ref} = 53^\circ$ (since here $\delta_F^d = 20^\circ$). The angle is then correctly regulated to the value $\phi_{ref} = 53^\circ$.



(a) Paths.

(b) Lateral deviation at T (veh. rear axle).

Figure 8: Experimental results.

In the following test, the objective consists to validate the control law proposed in subsection 3.2.2 for the stabilization of the vehicle-trailer system on a planned trajectory. To this aim, a 80m-long reference path was first recorded during a preliminary run achieved in manual driving with the mobile robot moving forward. Then, the path is autonomously

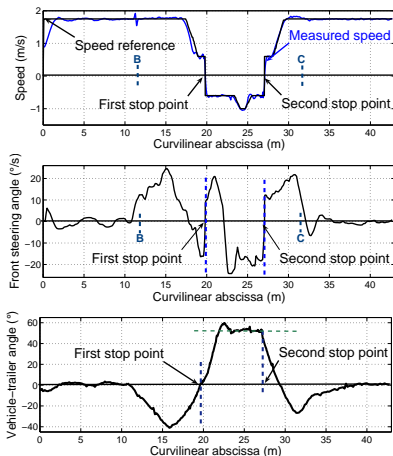


Figure 9: Speed, front steering angle, and ϕ .

followed backward at 0.5m/s with the vehicle-trailer system. At the beginning, the trailer starts with a lateral deviation of 1m from the path to be followed. Then, it reaches the planned path and maintains a satisfactory overall lateral error about $\pm 20\text{cm}$. Finally, the reverse turn maneuver depicted in figure 8(a) is performed with this control law. The lateral deviation, reported in figure 11, maintains an overall lateral error within $\pm 20\text{cm}$ during the maneuver.

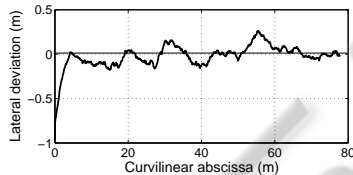


Figure 10: Reversing a vehicle-trailer system.

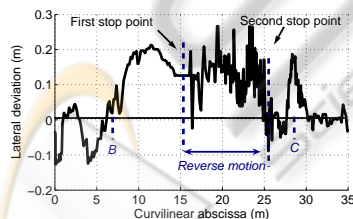


Figure 11: Lateral deviation at Q (trailer axle).

5 CONCLUSIONS

This paper addresses the problem of path generation and motion control for the autonomous maneuvers of a farm vehicle with a trailed implement in headland. A reverse turn planner has been first presented, based on primitives connected together with pieces of clothoid, in order to ensure curvature continuity.

Next, control algorithms have been considered. When the system is driving forward, the control algorithms are based on a kinematic model extended with additional sliding parameters and on model predictive control approaches. When the system is driving backward, two different steering controllers have been presented. Promising results are reported with an off-road mobile robot pulling a trailer during reverse turn maneuvers. In spite of a fast speed and high steering variations, an overall tracking error within $\pm 20\text{cm}$ is obtained during the maneuver.

REFERENCES

Altafi C., Speranzon A., W. B. (2001). A feedback control scheme for reversing a truck and trailer vehicle. In *IEEE Transactions on robotics and automation*, 17(6):915-922.

Cariou, C., Lenain, R., Thuilot, B., and Martinet, P. (2009). Motion planner and lateral-longitudinal controllers for autonomous maneuvers of a farm vehicle in headland. In *IEEE Intelligent Robots and Systems, St Louis, USA*.

Hermosillo J., S. S. (2003). Feedback control of a bi-steerable car using flatness: application to trajectory tracking. In *IEEE Int. American Control Conference, Denver, Co, USA*, 4:3567-3572.

Lamiroux F., L. J. (1998). A practical approach to feedback control for a mobile robot with trailer. In *IEEE Int. conf. on Robotics and Automation, Louvain, Belgique*.

Lau B., Sprunk C., B. W. (2009). Kinodynamic motion planning for mobile robots using splines. In *IEEE Intelligent Robots and Systems, St Louis, USA*.

Lenain, R., Thuilot, B., Cariou, C., and Martinet, P. (2006a). High accuracy path tracking for vehicles in presence of sliding: Application to farm vehicle automatic guidance for agricultural tasks. In *Autonomous Robots*, 21(1):79-97.

Lenain, R., Thuilot, B., Cariou, C., and Martinet, P. (2006b). Sideslip angles observer for vehicle guidance in sliding conditions: application to agricultural path tracking tasks. In *IEEE Int. conf. on Robotics and Automation, Orlando, USA*.

Vougioukas, S., Blackmore, S., Nielsen, J., and Fountas, S. (2006). A two-stage optimal motion planner for autonomous agricultural vehicles. In *Precision Agriculture*, 7:361-377.

Wang D., L. C. B. (2006). Modeling skidding and slipping in wheeled mobile robots: control design perspective. In *IEEE int. conf. on Intelligent Robots and Systems, Beijing, China*.